CONF-821037--30

DE83 001925

NEW METHOD FOR ANALYZING SMALL-SCALE FRACTURE-SPECIMEN DATA IN THE TRANSITION ZONE*

J. G. Merkle

Oak Ridge National Laboratory
Oak Ridge, Tennessee 37830

Among the problems related to the use of small specimens for measuring fracture toughness, those concerning size effects and data scatter are perennial. Figure 1 shows an early case encountered by the HSST Program. These data are from Compact Specimens of three different sizes, for an irradiated A508 Class 2 forging steel.[1] Later on, as shown in Fig. 2, substantial size effects and data scatter were encountered in the material characterization and experimental phases of HSST Thermal Shock Experiment TSE-5A. The line labeled K_{Ic} was drawn as a lower bound to the small specimen data before the test, but the actual test data, indicated by the solid triangles, fell below the line.[2]

Although the results shown in Fig. 2 were postulated to be statistical in nature, due to randomly dispersed brittle zones, metallographic examination failed to locate any such atypical regions.[3] In addition, a statistical approach to the problem of size effects and data scatter would be likely to require more specimens than are available in a surveillance capsule. Consequently, an attempt was made to find a suitable method for adjusting individual small specimen fracture toughness values for size effects in the transition range of temperature. The method selected was one already proposed by Irwin.[4] As illustrated in Fig. 3, taken from a study by Corten and Sailors,[5] Irwin's β_{Ic} equation recognizes an interaction between toughness and size. If either toughness increases or size decreases, the ratio K_c/K_{Ic} will increase. This interaction magnifies the scatter

*Research sponsored by the Office of Nuclear Regulatory Research, U.S. Nuclear Regulatory Commission under Interagency Agreements 40-551-75 and 40-552-75 with the U.S. Department of Energy under contract W-7405-eng-26 with the Union Carbide Corporation.

inherent in plane strain K_{Ic} values. Although the more common application of the β_{Ic} formula is the estimation of K_c values from known values of B and K_{Ic}, the original application[4] was the one considered here, i.e., the estimation of K_{Ic} from measured values of B and K_c. So the new aspect of the application described here is mainly the use of small specimen test data, analyzed inelastically.

An algebraic development of the β_{Ic} adjustment equation is described in Figs. 4 thru 6, and trial results, for both static and dynamic data, are shown in Figs. 7 thru 14. In Figs. 7 thru 14, the open points are the original small specimen toughness values, the closed points of the same shape are the corresponding β_{Ic} adjusted values, and the solid triangles are valid or large specimen test data. The appropriate ASME Code K_{Ic} or K_{IR} curves are shown for comparison. The original test data were obtained from References 2, and 6 thru 8.

The above results[9] are not without apparent contradiction, however.[10] Figure 15 shows that maximum load toughness values for A533-B steel plate show little data scatter or size effects. And as shown in Fig. 16, the same is true, with respect to data scatter, for the cylinder plate of HSST vessel V-9. However, Fig. 17 shows that the weld metal in vessels V-8 and V-9 develops considerable data scatter and size effects.[11] These observations concerning differences in the degree and scatter between plate, forgings and weld metal appear to be common, although unexplained.

The question of the presence or absence of size effects also appears to involve differences between plate and forgings, at least for static data. It also involves the definition of the toughness measurement point. Figure 10 shows definite size effects in static data at the point of cleavage instability, for A533-B steel, and their removal by applying the β_{Ic} formula. But Fig. 18 shows no appreciable size effects in the maximum load toughness values calculated for the same specimens,[10] although the final toughness values are higher in Fig. 18 than in Fig. 10. Fig. 19 shows the predictable results of applying the β_{Ic} adjustment to the A533-B plate maximum load data shown in Fig. 15, in which no appreciable size effects were evident. This size effect enigma is probably due in large part to the fact, illustrated in Fig. 20, that the maximum load point is often not the point of onset of

unstable cleavage. It is hypothesized here that, although enough microscopically stable cleavage microcracking[12, 13] occurrs to produce a temperature dependent maximum load toughness value, this value may not be a reliable K_{Ic} value because crack extension is predominantly by ductile tearing until the occurrence of unstable cleavage. This problem appears to be avoidable by using the point of onset of unstable cleavage as the toughness measurement point.

REFERENCES

1. J. A. Williams, "The Effect of Irradiation on the Fracture Toughness of A533-B Submerged-Arc Weld and A508, Class 2 Forging," *HSST Program Quarterly Progress Report for April–June 1974*, ORNL/TM-4655, Oak Ridge National Laboratory, Oak Ridge, Tenn., pp. 49–55.

2. R. D. Cheverton, *HSST Thermal-Shock Program Quick-Look Report for TSE-5A*, TSP-1007, Oak Ridge National Laboratory, Oak Ridge, Tenn., October 1980.

3. A. R. Rosenfield et al., "BCL HSST Support Program," *HSST Program Quarterly Progress Report for July–Sept. 1981*, ORNL/TM-8145, February 1982, pp. 10–43.

4. G. R. Irwin, "Fracture Mode Transition for a Crack Traversing a Plate," *J. of Basic Eng, ASME*, 82 (2), 417–425 (1960).

5. H. T. Corten and R H. Sailors, *Relationship Between Material Fracture Toughness Using Fracture Mechanics and Transition Temperature Tests*, T.&A.M. Report No. 346, Department of Theoretical and Applied Mechanics, University of Illinois, Urbana, Illinois, August, 1971.

6. T. Iwadate, Y. Tanaka, S. Ono and J. Watanabe, "An Analysis of Elastic-Plastic Fracture Toughness Behavior for J_{Ic} Measurement in the Transition Region," paper presented at the Second International Symposium on Elastic-Plastic Fracture Mechanics, Philadelphia, PA, October 6–9, 1981.

7. D. E. McCabe and J. D. Landes, *The Effect of Specimen Plan View Size and Material Thickness on the Transition Temperature of A533B Steel*, Research Report 80-1D3-REVEM-R2, Westinghouse R&D Center, Pittsburgh, PA, Nov. 1980.

8. F. J. Loss, "Dynamic Toughness Analysis of Pressure Vessel Steels," paper presented at the Third Water Reactor Safety Research Information Meeting, Gaithersburg, Maryland, September 29–October 2, 1975, (See also NRL Report 8006, U.S. Naval Research Laboratory, Washington, D.C., August 26, 1976, pp. 16–23.

9. J. G. Merkle, "Evaluation of Fracture Data from Small Specimens," presented at the Pressurized Thermal Shock Experiment Planning Review Meeting, Bethesda, Maryland, July 12-13, 1982.

10. F. J. Witt, unpublished discussion of Ref. 9, Westinghouse Electric Corp., Pittsburgh, PA., August 1982.

11. R. H. Bryan et al., *Test of 6-in.-Thick Pressure Vessels. Series 3: Intermediate Test Vessel V-8*, ORNL/NUREG-58, Oak Ridge National Laboratory, Oak Ridge, Tennessee, December 1979.

12. B. L. Averbach, "Physical Metallurgy and Mechanical Properties of Materials," Paper No. 2686, *J. Eng. Mech. Div., ASCE, EM 6*, 29–43 (1960).

13. F. J. Knott and A. H. Cottrell, "Notch Brittleness in Mild Steel," *J. Iron and Steel Inst.*, 249–260 (1963).

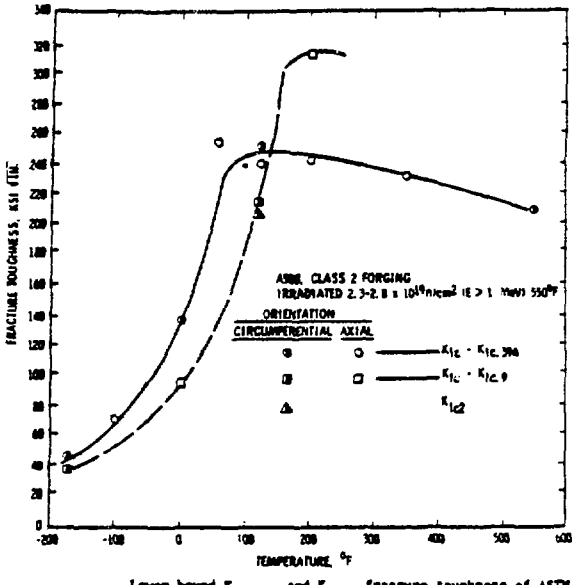

Lower bound $K_{Ic.394}$ and $K_{Ic.9}$ fracture toughness of ASTM A508, class 2 forging irradiated to 2.3–2.8 × 10^{19} n/cm² (E > 1 MeV) at 550°F. Both circumferential and axial orientations are shown.

FIGURE 1

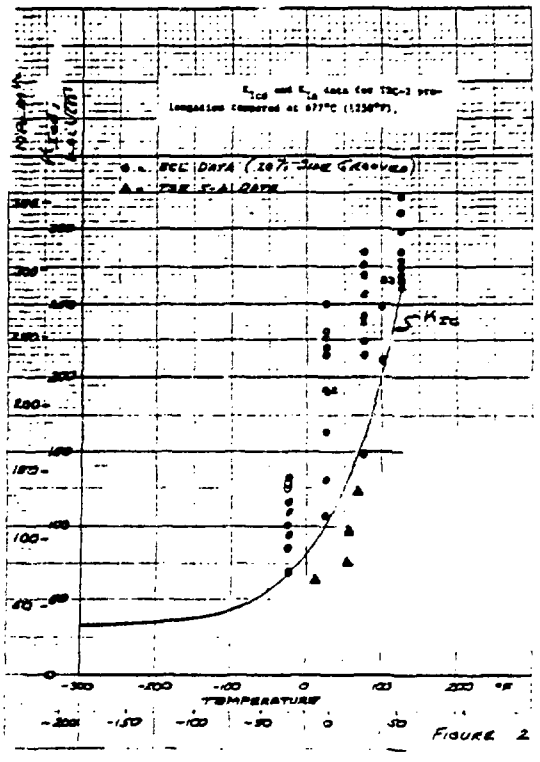

FIGURE 2

ILLUSTRATION OF THE APPLICATION OF THE IRWIN β_{I_a} THICKNESS ADJUSTMENT EQUATION

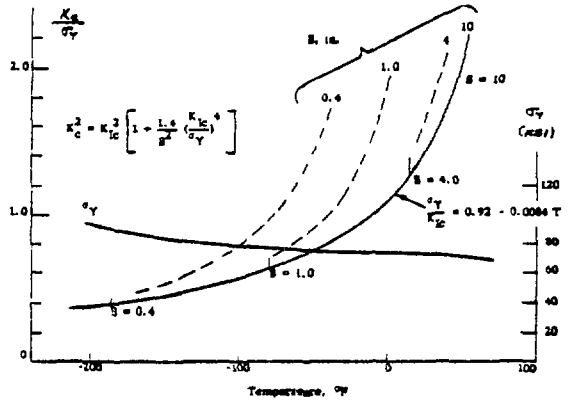

Illustration of "Thickness Fracture Mode Transition" Superimposed on "Fracture Micromechanism Transition" (Chaffin & Saibaba)

FIGURE 3

AN APPROACH TO THE DERIVATION AND APPLICATION OF IRWIN'S β_{I_a} EQUATION FOR ESTIMATING CONSTRAINT EFFECTS

DEFINITIONS:

K_{I_a} = PLANE STRAIN FRACTURE TOUGHNESS

K_a = NON PLANE STRAIN FRACTURE TOUGHNESS

EXPERIMENTAL OBSERVATIONS:

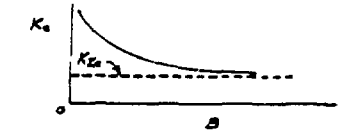

ANALYSIS

LET $\beta_{I_a} = \left(\frac{K_{I_a}}{\sigma_Y}\right)^2 \frac{1}{B}$ AND $\beta_a = \left(\frac{K_a}{\sigma_Y}\right)^2 \frac{1}{B}$

ASSUME

$$\beta_a = \beta_{I_a} + c\beta_{I_a}^3$$

(SIMPLEST NON-LINEAR ODD POWER POLYNOMIAL)

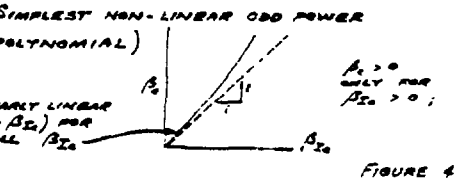

FIGURE 4

Evaluation of "c" at K_{Ic} Limit of Validity

$$A_1 = \beta_{I_a} + c\,\beta_{I_a}^3$$

$$c = \frac{\frac{A_1}{\beta_{I_a}} - 1}{\beta_{I_a}^2}$$

For complete plane strain

$$K_{I_a} = C\,\sigma_f \sqrt{\pi a_o}$$

(σ_f: plane strain fracture stress; a_o: original crack size)

Test result at limit of validity

$$K_c = C\,\sigma_f \sqrt{\pi a}$$

$$\therefore \quad \frac{A_1}{\beta_{I_a}} = \frac{\sigma_f^2}{\sigma_Y^2}\left(\frac{a}{a_o}\right)$$

Assume

$\frac{\sigma_f^2}{\sigma_Y^2} = 1.20$ (strain energy ratio)

$\frac{a}{a_o} = 1.02$ (see ASTM E-399)

Then $\frac{A_1}{\beta_{I_a}} = (1.20)(1.02) = 1.224$

Also, $B = 2.5\left(\frac{K_{I_a}}{\sigma_Y}\right)^2$, so $\beta_{I_a} = \frac{1}{2.5} = 0.4$

Therefore $c = \frac{1.224 - 1}{0.16} = \underline{1.4}$

Figure 5

Application of Irwin's β_{I_a} Equation

$$\beta_c = \beta_{I_a} + 1.4\,\beta_{I_a}^3$$

Calculation of K_c when K_{I_a} is known:

$$\frac{K_c}{K_{I_a}} = \sqrt{1 + 1.4\,\beta_{I_a}^2}$$

Calculation of K_{I_a} when K_c is known:

$$\beta_{I_a}^3 + \frac{5}{7}\beta_{I_a} - \frac{5}{7}\beta_c = 0$$

$$\beta_c = \frac{\left(\frac{K_c}{\sigma_Y}\right)^2}{B} \quad ; \quad \text{LET } m = \frac{5}{14}\beta_c$$

Note that $\frac{\left(\frac{5}{7}\right)^3}{27} = 0.0135$

$$A_1 = \sqrt{m^2 + 0.0135} + m$$

$$A_2 = \sqrt{m^2 + 0.0135} - m$$

$$\beta_{I_c} = A_1^{1/3} - A_2^{1/3}$$

$$K_{I_c} = K_c \sqrt{\frac{\beta_{I_a}}{\beta_c}}$$

Figure 6

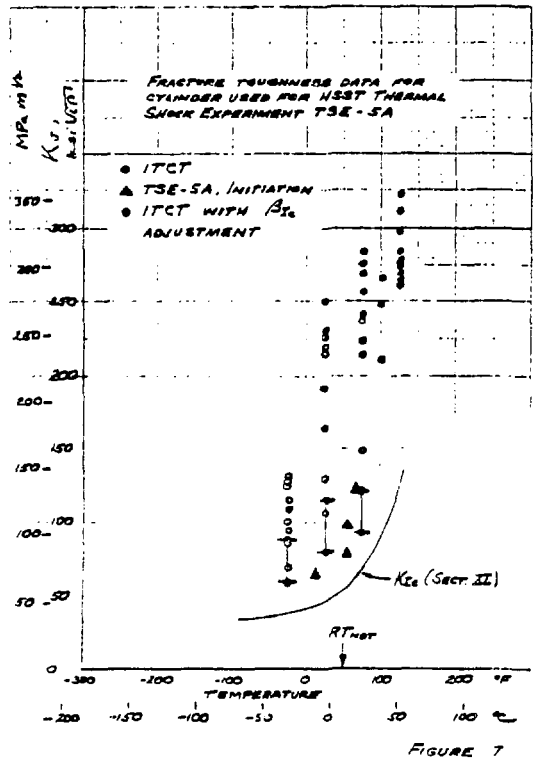

Figure 7

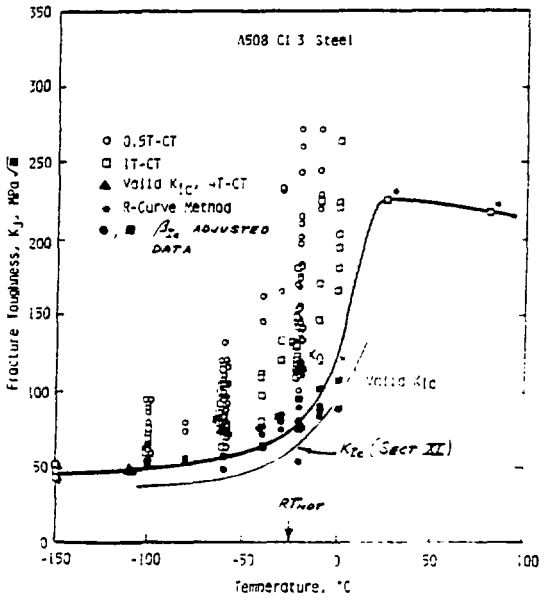

(Data from Iwabate et al.)

Figure 8

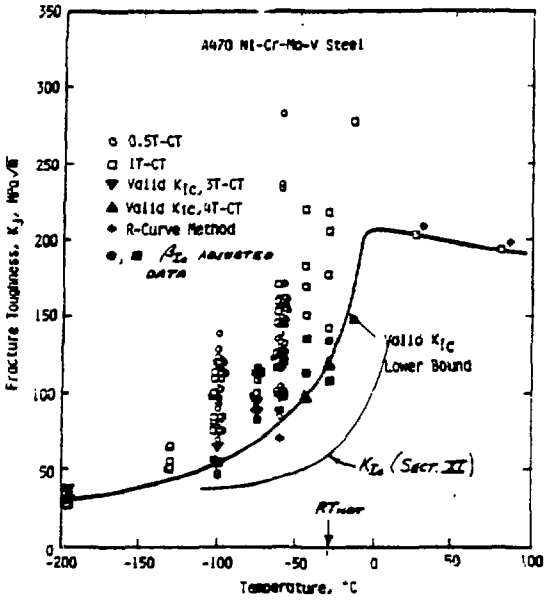

K_J for fracture calculated from Je versus temperature relation for A470 Ni-Cr-Mo-V rotor steel; (DATA FROM IWABATE ET AL).

FIGURE 9

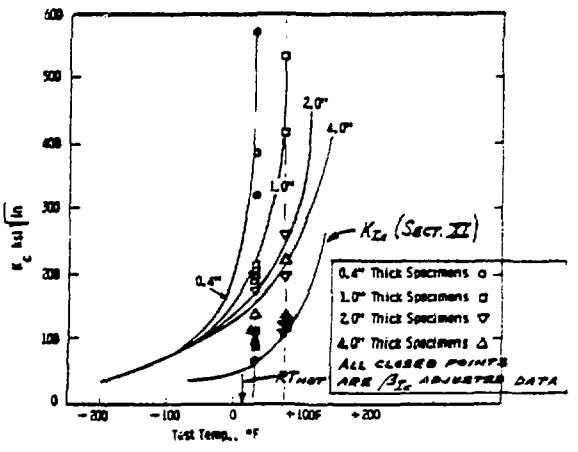

K_c instability versus test temperature separated by thicknesses scatter band of K_c instabilities (DATA FROM McCABE & LANDES)

FIGURE 10

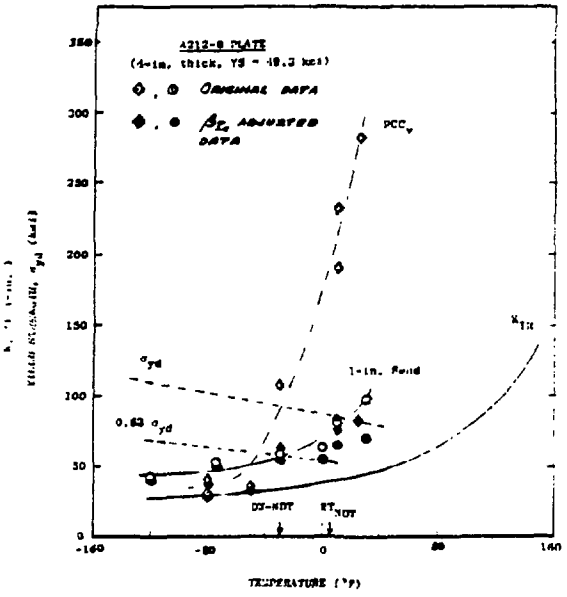

Comparison of dynamic fracture toughness trends for the A212-B reference plate. Both 1-in. bend and PCC_V specimens exhibited a $\dot{K}$ = 2.5×10⁵ ksi√in./sec. The open symbols represent fracture before cleavage initiation and the filled symbols [illegible] (DATA FROM LOSS).

FIGURE 11

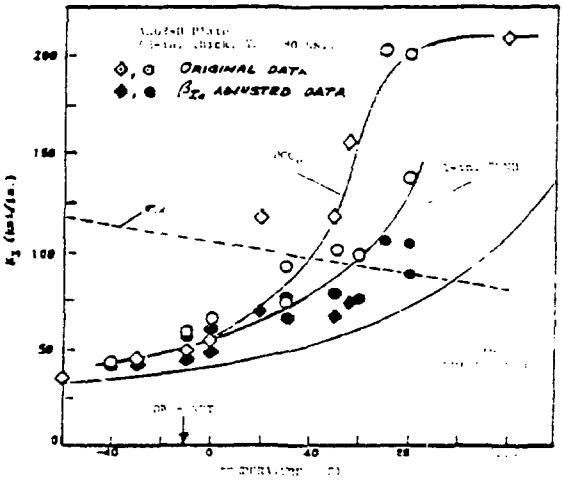

Comparison of dynamic fracture toughness trends for an A302-B plate. Both 1-in. bend and PCC_V specimens exhibited a $\dot{K}$ = 2.5 to 3×10⁵ ksi√in./sec. Data from Loss).

FIGURE 12

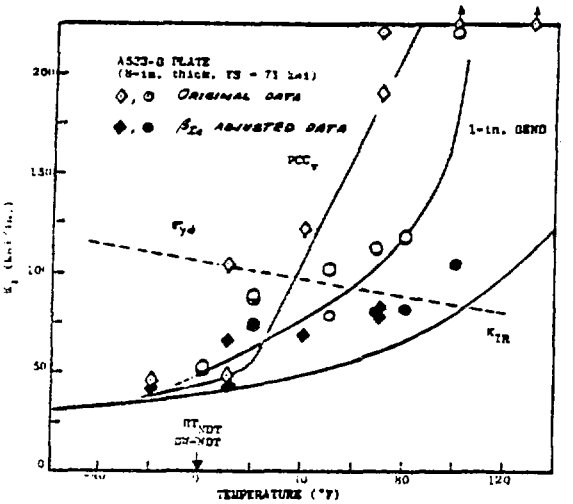

Comparison of dynamic fracture toughness trends for an A533-B Class 1 plate. Both 1-in. bend and PCC$_V$ specimens exhibited a $\dot{K}$ = 2.50 to 3×10^5 ksi√in. sec^{-1}. (Data from Lowe).

FIGURE 13

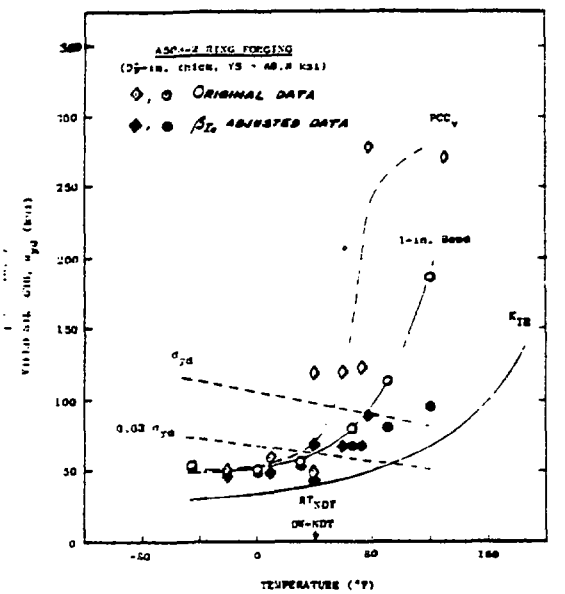

Comparison of dynamic fracture toughness trends for an A508 Class 2 forging. Both 1-in. bend and PCC$_V$ specimens exhibited a $\dot{K}$ 2.5×10^5 ksi√in. sec.$^{-1}$; (DATA FROM LOWE).

FIGURE 14

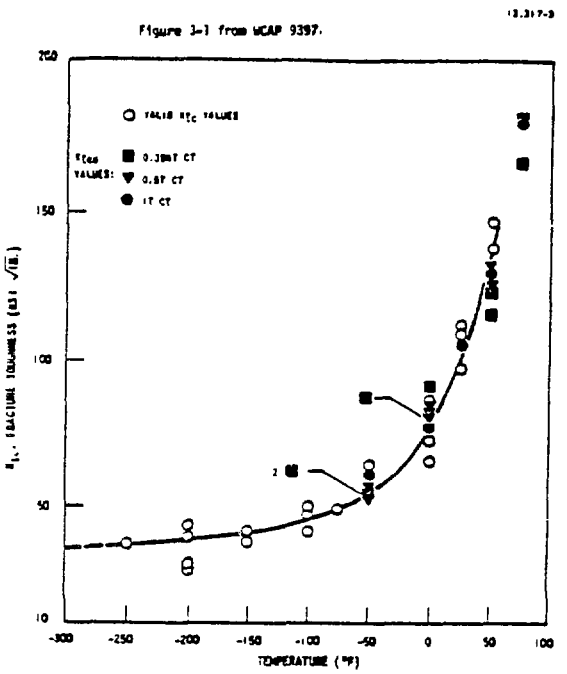

Figure C Comparison of Valid K_{Ic} Results in the Lower Transition Region with Lower Bound (K_{Ica}) Results Obtained for Charpy Thickness (0.394 in.), 0.5T and 1T Compact Specimens – A533 Grade B Class 1 Plate (HSST Plate 02)

FIGURE 15

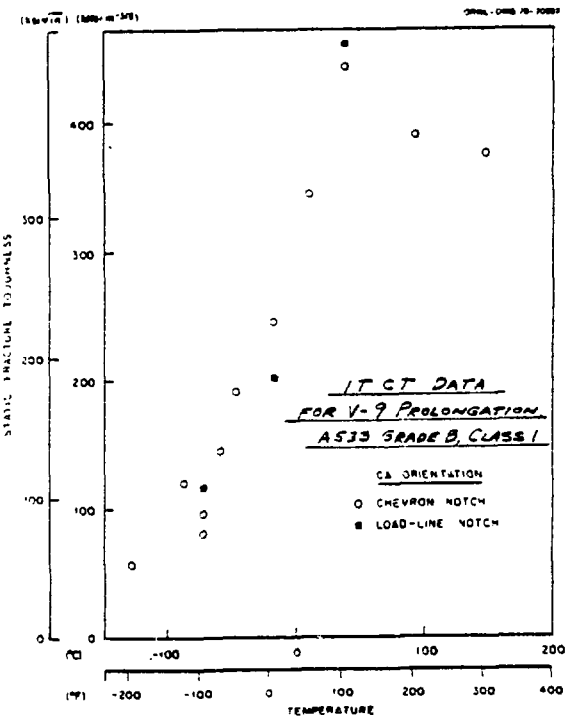

FIGURE 16

STATIC FRACTURE TOUGHNESS OF V-8 & V-9

PROLONGATION WELD METAL

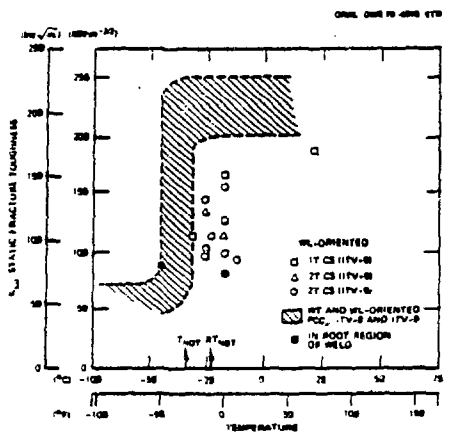

FIGURE 17

MAXIMUM LOAD K_{Icd} VALUES

FOR A533 GRADE B, CLASS 1, PLATE

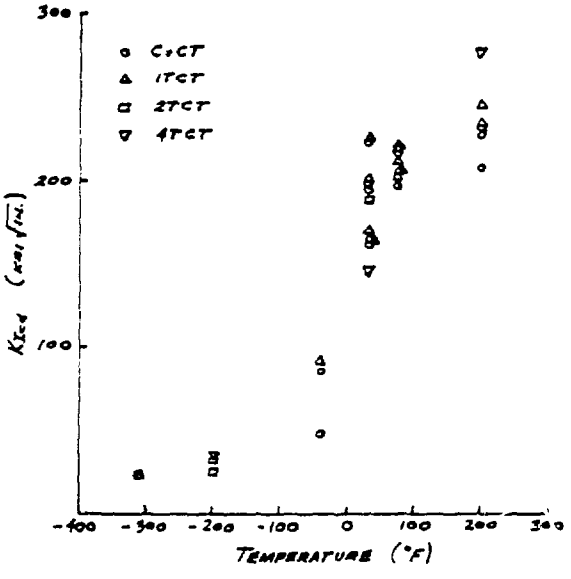

FIGURE 18

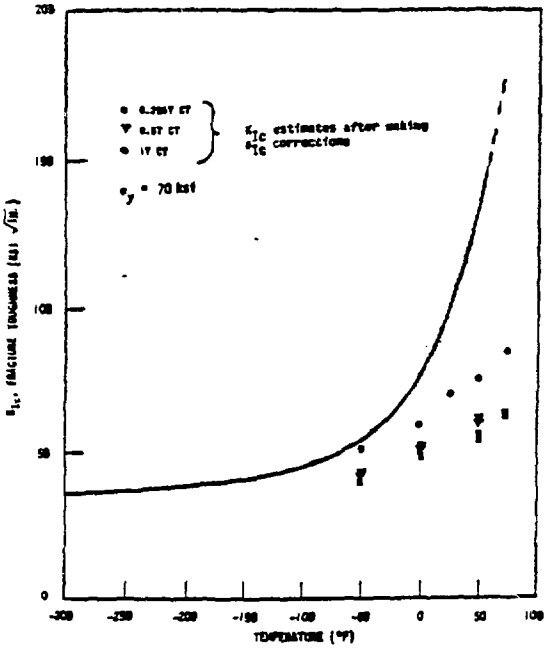

Figure 0 Comparison of K_{Ic} estimates using β_{Ic} correction with Valid K_{Ic} values (HSST Plate 02)

FIGURE 19

EXAMPLE OF A LOAD-DISPLACEMENT CURVE

FOR A SPECIMEN IN WHICH UNSTABLE CLEAVAGE

OCCURRED AFTER THE MAXIMUM LOAD POINT

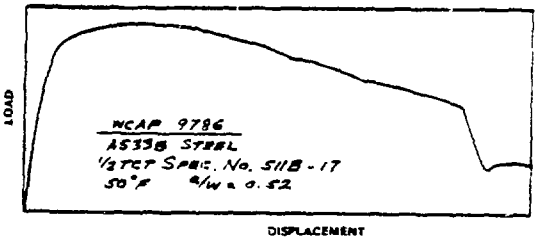

FIGURE 20